An autonomous polymerization motor powered by DNA hybridization

SUVIR VENKATARAMAN[1], ROBERT M. DIRKS[1], PAUL W. K. ROTHEMUND[2,3], ERIK WINFREE[2,3] AND NILES A. PIERCE[1,4]*

[1]Department of Bioengineering, California Institute of Technology, Pasadena, California 91125, USA
[2]Department of Computer Science, California Institute of Technology, Pasadena, California 91125, USA
[3]Department of Computation & Neural Systems, California Institute of Technology, Pasadena, California 91125, USA
[4]Department of Applied & Computational Mathematics, California Institute of Technology, Pasadena, California 91125, USA
*e-mail: niles@caltech.edu

Published online: 29 July 2007; doi:10.1038/nnano.2007.225

We present a synthetic molecular motor capable of autonomous nanoscale transport in solution. Inspired by bacterial pathogens such as *Rickettsia rickettsii*, which locomote by inducing the polymerization of the protein actin at their surfaces to form 'comet tails'[1], the motor operates by polymerizing a double-helical DNA tail[2]. DNA strands are propelled processively at the living end of the growing polymers, demonstrating autonomous locomotion powered by the free energy of DNA hybridization.

In recent years, the prospect of powering autonomous molecular machines by catalysing the hybridization of metastable DNA 'fuel' molecules has generated significant interest[3–6]. DNA is an attractive design material for engineering dynamic mechanical function, because the sequence of bases in each strand can be used to encode reaction pathways defined by prescribed hybridization interactions between segments of complementary bases[7,8]. However, despite the successful demonstration of several promising fuel systems[3–6], the goal of constructing an autonomous DNA locomotion device powered by hybridization has proven elusive. As an intermediate step, the free energy of hybridization has been used to fuel non-autonomous bipedal walkers that advance along DNA tracks powered by the manual sequential addition of auxiliary DNA fuel strands[9,10]. Taking a different approach altogether, autonomous locomotion of DNA-based systems has been achieved using other sources of energy, including hydrolysis of ATP or of the oligonucleotide backbone[11–14].

Here, we achieve autonomous locomotion by harnessing a hybridization chain reaction (HCR)[2] in which metastable DNA hairpins polymerize non-covalently when they encounter a target molecule. The driving force for this reaction is the formation of interstrand base pairs between previously unpaired bases in the polymerizing hairpins. Figure 1 depicts the proposed reaction pathway involving four species of DNA strands: hairpins H1 and H2, 'anchor' strand A and 'Rickettsia' strand R. A Rickettsia strand is propelled at the living end of the polymer away from its initial anchor strand partner, moving approximately 8 nm per polymerization step. Each polymerizing hairpin inserts itself between the Rickettsia strand and its polymer tail, performing a four-way branch migration (in which base pairs are exchanged between helices at a junction of four helices) that transfers the Rickettsia strand to the new living end. Throughout this process, the Rickettsia strand remains bound to the growing polymer by approximately 20 base pairs, thus ensuring processivity.

Native gel electrophoresis demonstrates that the hairpins do not polymerize in the absence of anchor/Rickettsia complexes (Fig. 2), that the anchor/Rickettsia complexes successfully initiate polymerization, and that the Rickettsia strands remain bound to the resulting polymers. Both the average and the width of the distribution of polymer lengths increase with time (see Supplementary Information, Fig. S1).

The processivity of Rickettsia transport was assessed by means of a capture experiment in which fluorescently labelled Rickettsia strands bound to anchor strands captured on beads were subjected to competitive polymerization in the presence of a large excess of unlabelled, uncaptured anchor/Rickettsia complexes (Fig. 3). If the Rickettsia (or anchor) strands dissociate transiently from their polymers during competitive polymerization, we would expect the eluate (the solution that remains after removing the beads) to be strongly fluorescent owing to partitioning of the labelled Rickettsias between captured polymers and the large excess of uncaptured polymers. Fluorescent eluate would also result if Rickettsias remain dissociated from polymers at equilibrium, or if polymer–polymer interactions contributed to the exchange of Rickettsia strands between polymers. The negligible fluorescence of the eluate following polymerization indicates that Rickettsia and anchor strands do not swap between polymers during polymerization. Furthermore, to confirm that the captured anchor/Rickettsia complexes underwent polymer growth during competitive polymerization, native gel electrophoresis was performed on the eluate following release of the captured species, revealing a distribution of polymer lengths (data not shown).

A fluorescence stepping experiment was then used to determine whether Rickettsia strands are propelled at the living end of the polymers. Starting with anchor strands complexed with dual-fluorescently labelled Rickettsia strands, we successively added excess unlabelled, excess quencher-labelled and excess unlabelled hairpins (Fig. 4). If the Rickettsia strands remain at the living end of the polymers during polymerization, we would expect to toggle the system between fully unquenched, fully quenched and fully unquenched states, as is observed. Gel electrophoresis after each hairpin addition step confirmed an

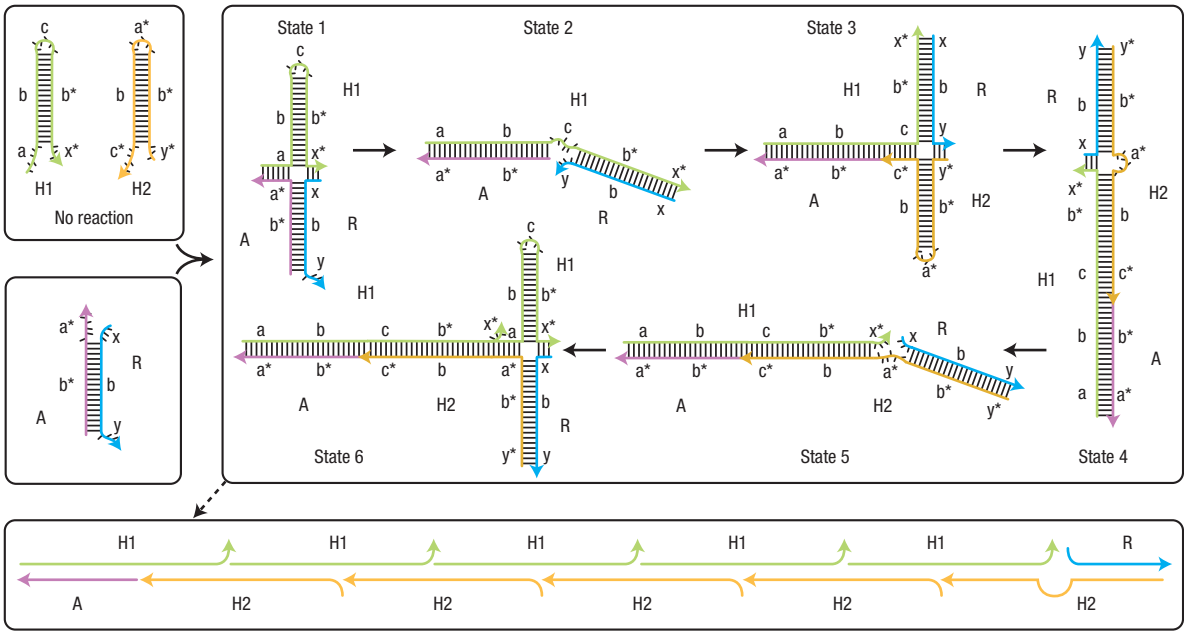

Figure 1 Mechanism schematic for a DNA-based Rickettsia mimic. The metastable fuel hairpins (H1 and H2) do not interact in the absence of the A·R complex (comprising anchor strand A and Rickettsia strand R). Upon mixing, H1 binds to the sticky ends of A·R (State 1), initiating a four-way branch migration in which R is passed from A to H1 (State 2). H2 then binds to the newly exposed sticky ends (State 3), initiating a four-way branch migration in which R is passed from H1 to H2 (State 4). Spontaneous breathing exposes sticky ends identical to those on the original A·R complex (State 5), allowing an H1 hairpin to bind and begin the next fuel cycle (State 6), continuing the hybridization chain reaction. In this manner, the R strand is passed back and forth between H1 and H2 hairpins at the living end of the growing polymer, moving away from the A strand, which remains bound to the initial H1 hairpin. Letters marked with a star identify sequence segments that are the reverse complement of segments identified by the corresponding unmarked letter. Here, the number of nucleotides in each strand segment are as follows: $|a| = |c| = 6$, $|b| = 18$, $|x| = |y| = 3$.

expected shift to longer polymer lengths (data not shown). Although fluorophores have sometimes been observed to cause off-pathway 'stuck states'[5,15], in the present case, the successful conversion between fully quenched and unquenched states appears to rule out this difficulty.

Direct observation of Rickettsia strand displacement away from the anchor strand was achieved using atomic force microscopy. Figure 5a depicts five polymers formed in solution using biotin-labelled anchor and Rickettsia strands. After deposition on mica, incubation with streptavidin revealed the location of the anchor and Rickettsia strands at either end of the polymers as dots in the image.

In summary, this battery of experiments demonstrates that the system behaves as designed, processively propelling the Rickettsia strand away from the anchor strand by carrying it at the living end of a polymer formed from metastable DNA hairpins. The polydispersity in polymer lengths evident in the gel data of Fig. 2 may now be interpreted to reflect polydispersity in the relative motion between the Rickettsia and anchor strands on a given polymer. Combined with the processivity result, it appears that for the longest observed polymers, a single Rickettsia strand can be robustly translated by dozens of 8-nm polymerization steps. The average speed of the Rickettsia strand relative to the anchor strand decreases with time and is on the order of nanometres per minute (see Supplementary Information, Fig. S1).

The invasive bacteria *Rickettsia rickettsii*, *Listeria monocytogenes* and *Shigella flexneri* exploit the polymerization of multiple actin filaments to generate sufficient force for locomotion at speeds on the order of micrometres per minute[1]. As a first step towards reproducing such behaviour in a purely nucleic acid system, here we demonstrate that multiple DNA polymerization motors grow

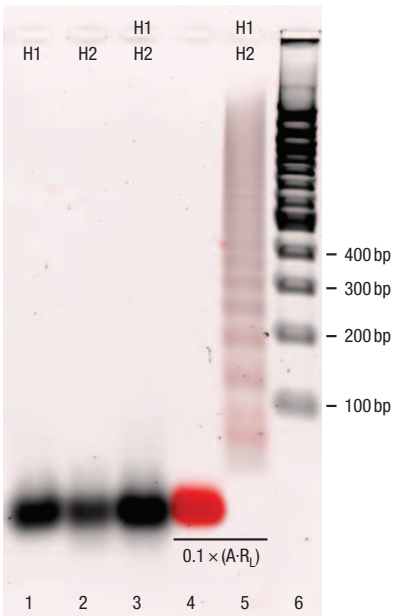

Figure 2 Fluorescent native agarose gel scanned at two wavelengths. Red channel: fluorophore Cy3 on the labelled strand R_L; black channel: staining of all species with SYBR Gold. The hairpins do not polymerize in the absence of A·R_L (lane 3). The A·R_L complex initiates polymerization of the hairpins and the labelled Rickettsia strand remains incorporated in the resulting polymers (lane 5). A 100-bp DNA ladder provides a reference for the migration of different helix lengths (lane 6). All samples are overnight reactions at room temperature with 1 μM hairpins.

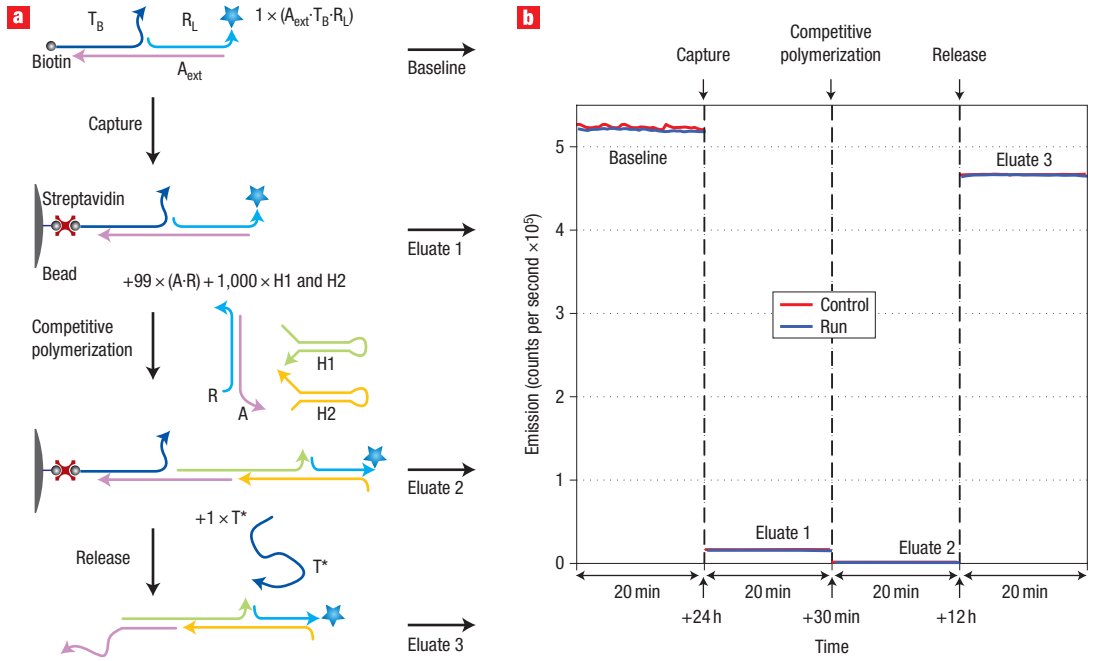

Figure 3 Fluorescence capture experiment demonstrating that during polymerization, each Rickettsia strand remains on the same polymer as its original anchor strand partner. a, Schematic defining the steps in the capture experiment. **b**, Fluorescence data for each step. Baseline: The fluorescence signal is obtained for complex $A_{ext} \cdot T_B \cdot R_L$ comprising an extended anchor strand, A_{ext}, bound to a 5′-biotin-labelled tether strand, T_B, and a 3′-Cy3-labelled Rickettsia strand, R_L. Eluate 1: The complexes are captured on streptavidin-coated beads by means of the biotin-labelled tethers; 97% of R_L strands are captured ($1 -$ (Eluate 1/Baseline)). Eluate 2: Competitive polymerization is performed by mixing the captured complexes with a 99-fold excess of unlabelled, untethered A·R complexes and a 1,000-fold excess of hairpins H1 and H2; only 0.3% of R_L strands are detected in the eluate (Eluate 2/Baseline). Eluate 3: Addition of the full reverse complement to the tether strand, T*, releases captured polymers; 92% of R_L strands are recovered (Eluate 3/Baseline). Controls omit hairpins and account for capture efficiency, blunt-end strand exchange, dilution and photobleaching. The total recovery (Eluates $[1 + 2 + 3]$/Baseline) is 95.5% for the run and 96.2% for the control.

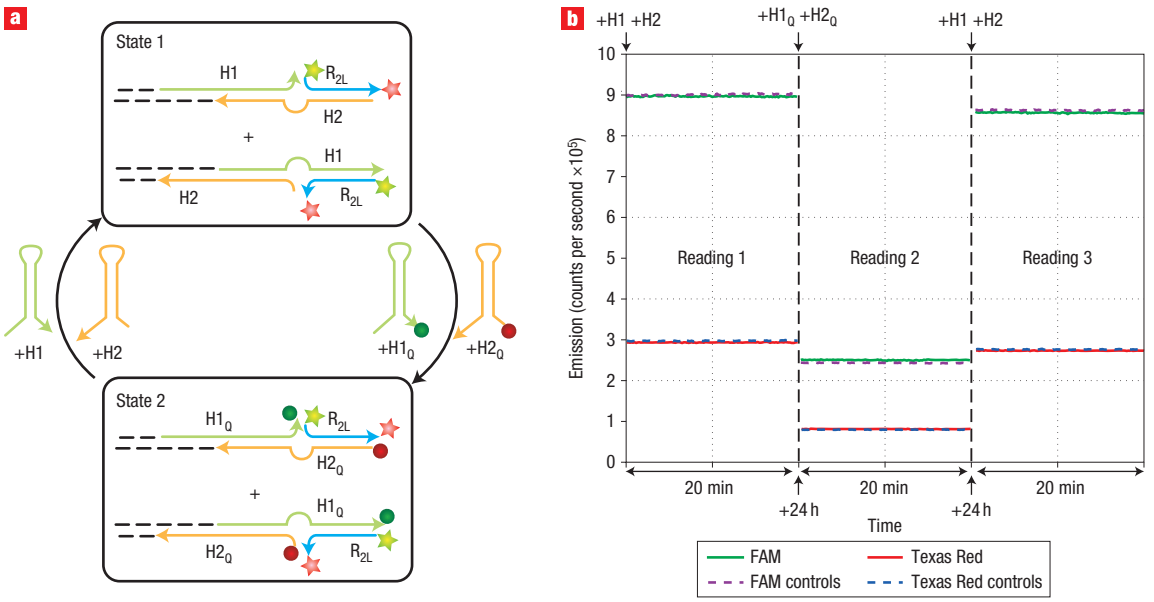

Figure 4 Fluorescence quenching experiment demonstrating that Rickettsia strands are carried at the live end of polymers. a, Schematic defining the states in the stepping experiment. **b**, Fluorescence readings. Reading 1: Polymerization is performed using unlabelled hairpins (600 pmol H1 and H2) and doubly labelled Rickettsia strands initially complexed with unlabelled anchor strands ($0.1 \times (A \cdot R_{2L})$, 5′ FAM, 3′ Texas Red), yielding polymers ending in either H1 or H2 (State 1). The control is identical in this case. Reading 2: Following addition of quencher hairpins (600 pmol $H1_Q$, 3′ BHQ1; 600 pmol $H2_Q$, 5′ IBRQ) and subsequent polymerization, the fluorescence signals in both channels drop to the fully quenched values of the control (for which the same steps are performed using quencher-labelled hairpins for all additions). This result suggests that polymers end in either $H1_Q$ or $H2_Q$, quenching both dyes on the R_{2L} strands (State 2). Reading 3: Following addition of unlabelled hairpins (600 pmol H1 and H2) and subsequent polymerization, both signals return to the fully unquenched values of the control (for which the same steps were performed using unlabelled hairpins for all additions). This result is consistent with a return to State 1.

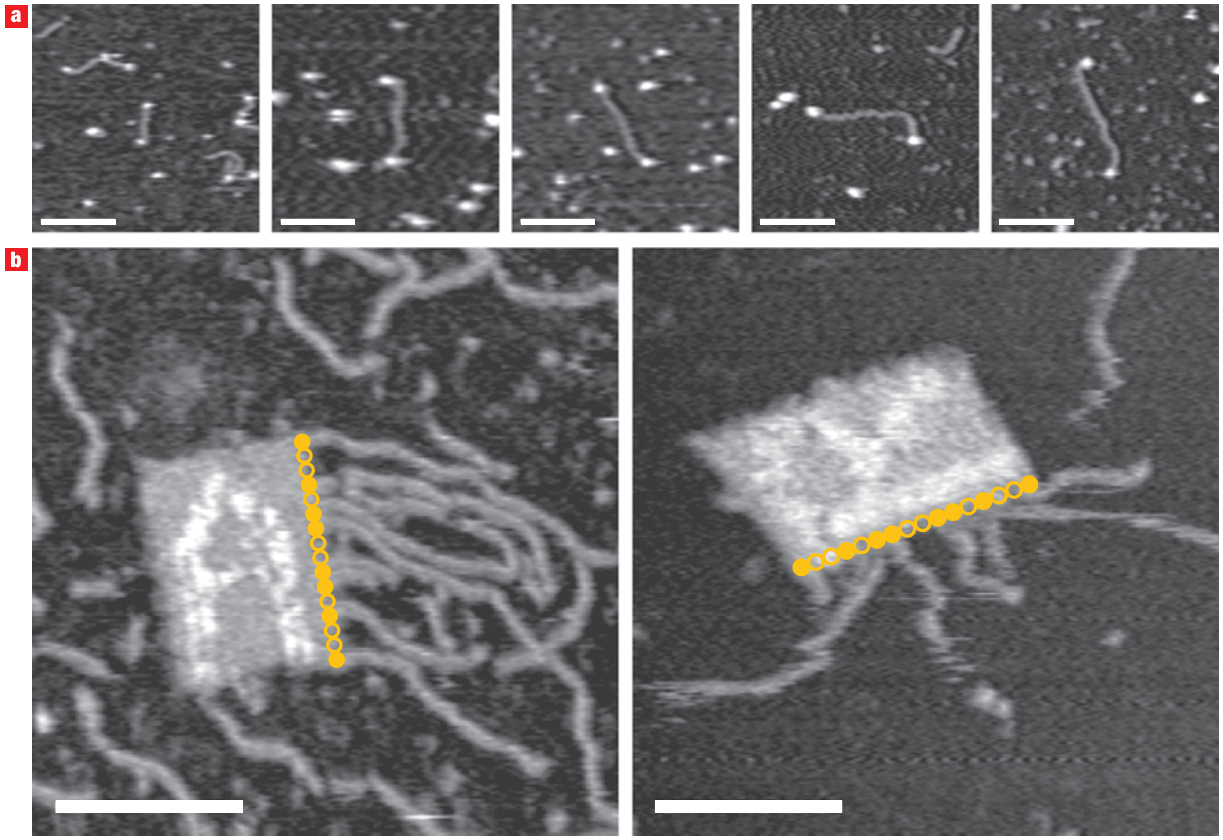

Figure 5 Direct visualization of Rickettsia systems by means of atomic force microscopy. a, Polymers with A and R strands at either end. Biotin-labelled anchor and Rickettsia strands were propelled apart by means of hairpin polymerization in solution and then deposited on mica, post-modified with streptavidin and imaged. From left to right, the approximate chain lengths for the polymers near the centre of each panel are 45 nm, 120 nm, 120 nm, 160 nm, and 165 nm, with each hairpin polmerization step corresponding to approximately 8 nm. **b**, Demonstration of spatial patterning of Rickettsia polymerization motors on the edge of 125 nm × 85 nm rectangular DNA origamis. The 'A' origami has eight anchor strands patterned on one side and thus polymer growth occurs at the distal end. The 'R' origami has eight Rickettsia strands patterned on one side and thus polymer growth occurs by insertion at the side of the origami. Closed circles denote sites that are expected to grow polymers; open circles denote sites that are expected to be free of polymers. Scale bars = 100 nm.

from DNA origami rectangles[16] into which anchor strands ('A origami') or Rickettsia strands ('R origami') have been incorporated in a prescribed pattern (Fig. 5b). For the R origami, polymerization occurs by insertion at the surface of the rectangle in geometric mimicry of the invasive bacteria. It remains to be seen whether multiple polymerizing tails of DNA are capable of propelling microscale objects freely through solution.

There are several interesting features in the Rickettsia design. The most striking feature is the ability of the Rickettsia strand to move from partner to partner while at every moment maintaining solid contact with the polymer. This is accomplished by using four-way branch migration to perform alternate handshakes with the H1 and H2 hairpins. To assist in the initiation of each four-way branch migration, the hairpins contain auxiliary sticky ends (x* and y* in Fig. 1), a strategy suggested by kinetic simulation studies[17] (J. M. Schaeffer, personal communication). By comparison, the original HCR scheme[2] used a cascade of three-way rather than four-way branch migrations. The reliance, here, on four-way branch migrations decreases the concentration of exposed single-stranded DNA in solution relative to alternative designs based on three-way branch migrations. We speculate that this strategy may represent a useful design principle that reduces the opportunity for off-pathway base-pairing and relaxes the requirements on sequence design quality. Finally, unlike previous DNA-based locomotion devices[9–14], no substrate or 'track' is required. It is intriguing, however, to envision Rickettsia-like systems growing polymer tails designed to function as tracks for other DNA-based locomotion devices.

The design of the Rickettsia system involved two stages. First, the locomotion mechanism was developed at the level of hairpin nucleation and branch migration steps using dimensions for each strand segment based on previous experience with hybridization chain reactions. Then, candidate sequences were obtained using a design algorithm (J. N. Zadeh, personal communication) that applied thermodynamic and kinetic criteria to a series of intermediate states drawn from the reaction pathway of Fig. 1 (see Methods). The experimental results demonstrate that these sequences encode a free-energy landscape with kinetic features (basins and the saddles that connect them) corresponding to the intended locomotion mechanism. It is conceptually significant that the system is closed, so that the function is autonomous. By comparison, non-autonomous concepts are simpler because they depend on the thermodynamic features of a sequence of free-energy landscapes, each defined by a different combination of user-controlled components. The present system provides a proof of principle that autonomous locomotion can be encoded in a

single free-energy landscape corresponding to a test tube of interacting DNA strands.

METHODS

SYSTEM SPECIFICATION

The DNA sequences for the four primary strands are:

H1: 5′/ATTCAAGCGACACCGTGGACGTGCACCCA CGCACGTCCACGGTGTCGCACC/3′
R: 5′/GGTGCGACACCGTGGACGTGCAAC/3′
H2: 5′/GTTGCACGTCCACGGTGTCGCTTGAATGCGA CACCGTGGACGTGCGTGGGT/3′
A: 5′/GCACGTCCACGGTGTCGCTTGAAT/3′

For the fluorescence stepping experiments R was replaced by R_{2L}, which is labelled on the 5′ end with 6-carboxyfluorescein (FAM) and on the 3′ end with Texas Red-X NHS Ester. For the fluorescence capture experiments R was replaced by R_L, which is labelled on the 5′ end with Cy3, and A was extended by 18 nucleotides, to make A_{ext}. Additional modified hairpins were also used: $H1_Q$ is H1 labelled with Black Hole Quencher 1 (BHQ1) on the 3′ end and $H2_Q$ is H2 labelled with Iowa Black RQ (IBRQ) quencher on the 5′ end. Two additional strands were also used for the capture experiment: a tether strand (T), which was biotin-labelled on the 5′ end, and its reverse complement T*.

A_{ext}: 5′/GCACGTCCACGGTGTCGCTTGAATGCGAACG ACGAGCTGAAG/3′
T: 5′/ACCAGACTTCAGCTCGTCGTTCGCTACTAGACTCCG/3′
T*: 5′/CGGAGTCTAGTAGCGAACGACGAGCTGAAGTCTGGT/3′

DNA oligomers were synthesized, labelled and purified (PAGE for A, A_{ext}, R, H1, H2, T, T*; HPLC for R_L, R_{2L}, $H1_Q$, $H2_Q$) by Integrated DNA Technologies.

SEQUENCE DESIGN

Sequences were optimized based on both thermodynamic and kinetic criteria. First, thermodynamic optimization was performed by considering a set of target secondary structures involving different subsets of the strands (H1, H2, A·R, H1·R·A (Fig. 1, State 2) and H1·R·H2·A (Fig. 1, State 4)). Affinity and specificity for these structures were optimized simultaneously by calculating the average number of incorrectly paired bases at equilibrium for each target structure[18] and mutating the sequences to minimize the sum of this quantity over all of the target structures (J. N. Zadeh, personal communication).

After obtaining a large set of candidate sequences that appeared promising on thermodynamic grounds, we performed stochastic kinetic simulations[17] to identify those sequences that are predicted to proceed most rapidly along the intended reaction pathways (J. M. Schaeffer, personal communication). Median first passage times were computed from the minimum free-energy (MFE) structures of H1, H2 and the A·R complex, to the computed MFE structures of H2 and the H1·R·A complex (Fig. 1, State 2) and then to the computed MFE structure of the H1·L·H2·R complex (Fig. 1, State 4). The sequences selected for experimental study were predicted to behave well on both thermodynamic and kinetic evaluation criteria.

Received 14 March 2007; accepted 27 June 2007; published 29 July 2007.

References

1. Gouin, E., Welch, M. D. & Cossart, P. Actin-based motility of intracellular pathogens. *Curr. Opin. Microbiol.* **8,** 35–45 (1999).
2. Dirks, R. M. & Pierce, N. A. Triggered amplification by hybridization chain reaction. *Proc. Natl Acad. Sci. USA* **101,** 15275–15278 (2004).
3. Turberfield, A. J. *et al.* DNA fuel for free-running nanomachines. *Phys. Rev. Lett.* **90,** 118102 (2003).
4. Bois, J. S. *et al.* Topological constraints in nucleic acid hybridization kinetics. *Nucleic Acids Res.* **33,** 4090–4095 (2005).
5. Seelig, G., Yurke, B. & Winfree, E. Catalyzed relaxation of a metastable DNA fuel. *J. Am. Chem. Soc.* **128,** 12211–12220 (2006).
6. Green, S. J., Lubrich, D. & Turberfield, A. J. DNA hairpins: fuel for autonomous DNA devices. *Biophys. J.* **91,** 2966–2975 (2006).
7. Seeman, N. C. From genes to machines: DNA nanomechanical devices. *Trends Biochem. Sci.* **30,** 119–125 (2005).
8. Simmel, F. C. & Dittmer, W. U. DNA nanodevices. *Small* **1,** 284–299 (2005).
9. Sherman, W. B. & Seeman, N. C. A precisely controlled DNA biped walking device. *Nano Lett.* **4,** 1203–1207 (2004).
10. Shin, J.-S. & Pierce, N. A. A synthetic DNA walker for molecular transport. *J. Am. Chem. Soc.* **126,** 10834–10835 (2004).
11. Yin, P., Yan, H., Daniell, X. G., Turberfield, A. J. & Reif, J. H. A unidirectional DNA walker that moves autonomously along a track. *Angew. Chem. Int. Edn* **43,** 4906–4911 (2004).
12. Tian, Y., He, Y., Chen, Y., Yin, P. & Mao, C. A DNAzyme that walks processively and autonomously along a one-dimensional track. *Angew. Chem. Int. Edn* **44,** 2–5 (2005).
13. Bath, J., Green, S. J. & Turberfield, A. J. A free-running DNA motor powered by a nicking enzyme. *Angew. Chem. Int. Edn* **44,** 4358–4361 (2005).
14. Pei, R. *et al.* Behavior of polycatalytic assemblies in a substrate-displaying matrix. *J. Am. Chem. Soc.* **128,** 12693–12699 (2006).
15. Marras, S. A. E., Kramer, F. R. & Tyagi, S. Efficiencies of fluorescence resonance energy transfer and contact-mediated quenching in oligonucleotide probes. *Nucleic Acids Res.* **30,** e122 (2002).
16. Rothemund, P. W. K. Folding DNA to create nanoscale shapes and patterns. *Nature* **440,** 297–302 (2006).
17. Flamm, C., Fontana, W., Hofacker, I. L. & Schuster, P. RNA folding at elementary step resolution. *RNA* **6,** 325–338 (2000).
18. Dirks, R. M., Lin, M., Winfree, E. & Pierce, N. A. Paradigms for computational nucleic acid design. *Nucleic Acids Res.* **32,** 1392–1403 (2004).

Acknowledgements

We thank J. S. Bois for helpful discussions, J. Padilla for performing the early sequence design calculations, J. N. Zadeh for the use of unpublished multi-objective sequence design software, J. M. Schaeffer for the use of unpublished multi-stranded kinetics simulation software and R. Barish and R. Hariadi for guidance on the use of DNA origamis for patterning polymerization reactions. This work was funded by NSF-CCF-CAREER-0448835, NSF-CHE-0533064 (Center for Molecular Cybernetics), NSF-CCF-0622254, NSF-DMS-0506468.
Correspondence and requests for materials should be addressed to N.A.P.
Supplementary information accompanies this papers at www.nature.com/naturenanotechnology

Competing financial interests

The authors declare no competing financial interests.